Hybrid Precoders and Combiners for mmWave MIMO Systems with Per-Antenna Power Constraints

R. López-Valcarce*, N. González-Prelcic*, C. Rusu*
Universidade de Vigo, Vigo, Spain
Email: {valcarce,nuria,crusu}@gts.uvigo.es

R. W. Heath, Jr.†
The University of Texas at Austin, USA
Email: rheath@utexas.edu

***Abstract*—This paper considers the design of hybrid precoders and combiners for mmWave MIMO systems with per-antenna power constraints and the additional limitations introduced by the phase-shifting network in the analog processing stage. Previous hybrid designs were obtained using a total power constraint, but in practical implementations per-antenna constraints are more realistic, specially at mmWave, given the large number of power amplifiers used in the transmit array. Assuming perfect channel knowledge, we obtain first an approximation to the all-digital solution for the precoder and the combiner given the per-antenna constraints. Then, we develop a new method for the design of the hybrid precoder and combiner which attempts to match such all-digital approximation. Simulation results show the effectiveness of the proposed approach, which performs close to the all-digital solution.**

I. Introduction

Hybrid precoding is a MIMO architecture that reduces cost and power consumption of large antenna arrays in mmWave MIMO systems, by partitioning the spatial processing into the analog RF and digital baseband (BB) domains [1], [2]. Since the pioneering work in [3], many different designs have been proposed [4]–[10]. These approaches achieve high spectral efficiency, close to that of the all-digital solution [11] when a narrowband clustered channel model is considered. All these designs are obtained assuming a constraint on the total transmit power. Per-antenna power constraints, though, are more realistic, since each antenna element in the transmit array is equipped with its own power amplifier. This is particularly important in mmWave systems, in which the array comprises a much larger number of antennas and amplifiers than in conventional cellular systems.

The design of optimal precoders and combiners maximizing spectral efficiency for a conventional (all-digital) MIMO system subject to per-antenna power constraints has not been clearly solved in the previous literature. The work in [12], [13] considers the maximization of the mutual information with per-antenna power constraints in a multistream single user MIMO system. To this end, an iterative approach is proposed for the design of the optimal precoder. Since the focus was on mutual information, the design of the combiner was not addressed in [12], [13]. As shown in [14], maximizing the mutual information amounts to minimizing the determinant of the error covariance matrix, assuming a minimum Mean Squared Error linear receiver.

Alternative criteria other than spectral efficiency have also been considered for all-digital MIMO transceivers under per-antenna power constraints. In [15], the precoder and combiner are chosen to maximize the receive SNR, whereas [16] proposes an MMSE precoder design minimizing the bit error rate of the single-user MIMO system. The multiuser MIMO setting with per-antenna power constraints was considered in [17], seeking the optimum precoder and combiner to maximize SINR for the different streams. The downlink channel in a multiuser system is also considered in [18], where the maximum transmit power on each transmit antenna is minimized, subject to per-user SINR constraints.

In this paper, we develop hybrid precoders and combiners with per-antenna power constraints for mmWave systems, in which the RF analog processing is implemented by means of phase shifters. Whereas previous hybrid transceiver designs consider the maximization of the mutual information, thus decoupling the designs of the precoder and the combiner, and with a total power constraint, we address the maximization of the spectral efficiency by jointly designing the precoder and combiner under per-antenna constraints. To this end, we first consider an all-digital design without any hardware-related constraints. Since the resulting problem is difficult, we introduce a relaxation leading to a suboptimal solution that can be obtained in closed form. Once the jointly optimum precoder and combiner for the relaxed problem are obtained, we propose a heuristic strategy to cope with the hardware limitations of the analog RF stages. We obtain first an approximation of the RF precoder, optimizing the baseband precoder in a second stage. The combiner is designed using a similar approach. Simulation results show that the spectral efficiency achieved by the hybrid design is very close to that of the all-digital solution, while satisfying at the same time the individual per-antenna constraints.

*Supported by the Spanish Government and the European Regional Development Fund (ERDF) (TEC2013-47020-C2-1-R COMPASS, TEC2015-69648-REDC Red COMONSENS) and the Galician Government and ERDF (GRC2013/009, R2014/037 REdTEIC and AtlantTIC).

†Supported in part by the National Science Foundation under Grant No. NSF-CCF-1319556 and NSF-CCF-1527079.

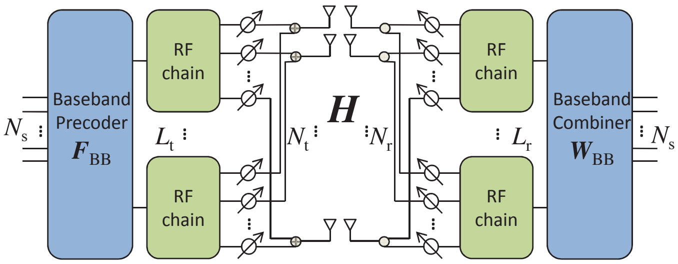

Fig. 1. Single-user mmWave hybrid system architecture.

II. System Model

Consider a single-user mmWave MIMO system as shown in Fig. 1. The transmit terminal is equipped with N_{t} transmit antennas and $L_{\mathrm{t}} \leq N_{\mathrm{t}}$ RF chains, whereas the receive terminal has N_{r} antennas and $L_{\mathrm{r}} \leq N_{\mathrm{r}}$ RF chains. A total of N_{s} data streams are to be transmitted, with $N_{\mathrm{s}} \leq \min\{L_{\mathrm{t}}, L_{\mathrm{r}}\}$.

At the transmitter, a linear precoder $\boldsymbol{F} \in \mathbb{C}^{N_{\mathrm{t}} \times N_{\mathrm{s}}}$ is applied to the symbol vector $\boldsymbol{s} \in \mathbb{C}^{N_{\mathrm{s}}}$, with $\mathbb{E}[\boldsymbol{s}\boldsymbol{s}^*] = \frac{1}{N_{\mathrm{s}}}\boldsymbol{I}_{N_{\mathrm{s}}}$. The precoder output $\boldsymbol{x} = \boldsymbol{F}\boldsymbol{s}$ is sent over a narrowband, block-fading channel. Assuming perfect carrier and timing synchronization, the received signal can be written as

$$\boldsymbol{r} = \sqrt{\rho}\boldsymbol{H}\boldsymbol{F}\boldsymbol{s} + \boldsymbol{n}, \tag{1}$$

where $\boldsymbol{H} \in \mathbb{C}^{N_{\mathrm{r}} \times N_{\mathrm{t}}}$ is the channel matrix with $\mathbb{E}[\|\boldsymbol{H}\|_F^2] = N_{\mathrm{t}}N_{\mathrm{r}}$, ρ denotes the average transmit power per symbol, and $\boldsymbol{n} \in \mathbb{C}^{N_{\mathrm{r}}}$ is the zero-mean Gaussian noise vector with $\mathbb{E}[\boldsymbol{n}\boldsymbol{n}^*] = \boldsymbol{I}_{N_{\mathrm{r}}}$. Since the noise has unit variance, ρ can be identified with the signal-to-noise ratio (SNR).

The receiver applies a linear combiner $\boldsymbol{W} \in \mathbb{C}^{N_{\mathrm{r}} \times N_{\mathrm{s}}}$ to the received signal in order to obtain

$$\boldsymbol{y} = \boldsymbol{W}^*\boldsymbol{r} = \sqrt{\rho}\boldsymbol{W}^*\boldsymbol{H}\boldsymbol{F}\boldsymbol{s} + \boldsymbol{W}^*\boldsymbol{n}. \tag{2}$$

A hybrid architecture is assumed for the precoder and the combiner. The hybrid precoder $\boldsymbol{F} = \boldsymbol{F}_{\mathrm{RF}}\boldsymbol{F}_{\mathrm{BB}}$ consists of a baseband precoder $\boldsymbol{F}_{\mathrm{BB}} \in \mathbb{C}^{L_{\mathrm{t}} \times N_{\mathrm{s}}}$ followed by an RF precoder $\boldsymbol{F}_{\mathrm{RF}} \in \mathbb{C}^{N_{\mathrm{t}} \times L_{\mathrm{t}}}$. Analogously, the hybrid combiner $\boldsymbol{W} = \boldsymbol{W}_{\mathrm{RF}}\boldsymbol{W}_{\mathrm{BB}}$ is composed of an RF combiner $\boldsymbol{W}_{\mathrm{RF}} \in \mathbb{C}^{N_{\mathrm{r}} \times L_{\mathrm{r}}}$ and a baseband combiner $\boldsymbol{W}_{\mathrm{BB}} \in \mathbb{C}^{L_{\mathrm{r}} \times N_{\mathrm{s}}}$. Since the RF precoder and combiner are implemented in the analog domain, they are subject to hardware-specific constraints. In particular, we assume that $\boldsymbol{F}_{\mathrm{RF}}$ and $\boldsymbol{W}_{\mathrm{RF}}$ are implemented with a network of variable analog phase shifters, so that every entry in these matrices has unit magnitude.

III. Problem Formulation

Assuming perfect channel state information at the transmitter and receiver, the problem considered is to design the hybrid precoder and combiner to maximize the spectral efficiency. If we define the effective channel and the noise covariance matrix after combining, respectively, as

$$\boldsymbol{H}_{\mathrm{e}} \triangleq \boldsymbol{W}^*\boldsymbol{H}\boldsymbol{F} = \boldsymbol{W}_{\mathrm{BB}}^*\boldsymbol{W}_{\mathrm{RF}}^*\boldsymbol{H}\boldsymbol{F}_{\mathrm{RF}}\boldsymbol{F}_{\mathrm{BB}}, \tag{3}$$

$$\boldsymbol{R}_{\mathrm{e}} \triangleq \boldsymbol{W}^*\boldsymbol{W} = \boldsymbol{W}_{\mathrm{BB}}^*\boldsymbol{W}_{\mathrm{RF}}^*\boldsymbol{W}_{\mathrm{RF}}\boldsymbol{W}_{\mathrm{BB}}, \tag{4}$$

then the spectral efficiency can be written as

$$\mathcal{R}(\boldsymbol{F}, \boldsymbol{W}) = \log_2\left|\boldsymbol{I}_{N_{\mathrm{s}}} + \frac{\rho}{N_{\mathrm{s}}}\boldsymbol{H}_{\mathrm{e}}^*\boldsymbol{R}_{\mathrm{e}}^{-1}\boldsymbol{H}_{\mathrm{e}}\right|. \tag{5}$$

We consider individual power constraints at each of the N_{t} transmit antennas:

$$\boldsymbol{e}_j^*\boldsymbol{F}\boldsymbol{F}^*\boldsymbol{e}_j \leq p_j, \qquad j = 1, \ldots, N_{\mathrm{t}}, \tag{6}$$

where $\boldsymbol{e}_j$ denotes the j-th element of the standard basis, and $p_j > 0$ is the available average power at the j-th transmit antenna, $j = 1, \ldots, N_{\mathrm{t}}$. In addition, the hardware-specific constraints

$$\boldsymbol{F}_{\mathrm{RF}} \in \mathcal{M}^{N_{\mathrm{t}} \times L_{\mathrm{t}}}, \qquad \boldsymbol{W}_{\mathrm{RF}} \in \mathcal{M}^{N_{\mathrm{r}} \times L_{\mathrm{r}}} \tag{7}$$

must hold as well, where $\mathcal{M}^{m \times n}$ denotes the set of $m \times n$ matrices with unit-magnitude entries.

To get some insight about hybrid precoder and combiner design, we will study first the corresponding problem in which the hardware-specific constraints (7) are removed.

IV. All-digital design

Assume for the moment an all-digital implementation of the precoder and combiner, and consider the problem of jointly maximizing $\mathcal{R}(\boldsymbol{F}, \boldsymbol{W})$ directly with respect to $\boldsymbol{F}$ and $\boldsymbol{W}$ subject to the per-antenna power constraints (6). A related problem was considered in [13], namely the maximization with respect to $\boldsymbol{F}$ of the mutual information

$$\mathcal{I}(\boldsymbol{F}) = \log_2\left|\boldsymbol{I}_{N_{\mathrm{s}}} + \frac{\rho}{N_{\mathrm{s}}}\boldsymbol{F}^*\boldsymbol{H}^*\boldsymbol{H}\boldsymbol{F}\right|, \tag{8}$$

subject to the constraints (6). There, an iterative algorithm was proposed to compute the optimal precoder; it was also shown in [13] that such optimal precoder must satisfy all per-antenna power constraints (6) with equality. This result can be extended as follows (see Appendix A for the proof):

Lemma 1. *Consider the problem*

$$\max_{\boldsymbol{F},\boldsymbol{W}} \mathcal{R}(\boldsymbol{F}, \boldsymbol{W}) \quad \text{s. to} \quad \boldsymbol{e}_j^*\boldsymbol{F}\boldsymbol{F}^*\boldsymbol{e}_j \leq p_j, \quad j = 1, \ldots, N_{\mathrm{t}}. \tag{9}$$

Then the optimal precoder for (9) *satisfies all the per-antenna power constraints with equality.*

Since the solution to problem (9) is difficult to characterize beyond the result in Lemma 1, we resort to suboptimal but tractable approximations. For this, note that the average power at any transmit antenna can be upper bounded as

$$\boldsymbol{e}_j^*\boldsymbol{F}\boldsymbol{F}^*\boldsymbol{e}_j \leq \sigma_1^2(\boldsymbol{F}), \tag{10}$$

where $\sigma_1(\boldsymbol{F})$ denotes the largest singular value of $\boldsymbol{F}$ (it constitutes the *spectral norm* of $\boldsymbol{F}$). Hence, if we let $p_0 \triangleq \min_j\{p_j\}$, then the set of precoders satisfying $\sigma_1^2(\boldsymbol{F}) \leq p_0$ is feasible for problem (9). Consider now the following "relaxed" problem:

$$\max_{\boldsymbol{F},\boldsymbol{W}} \mathcal{R}(\boldsymbol{F}, \boldsymbol{W}) \quad \text{s. to} \quad \sigma_1^2(\boldsymbol{F}) \leq p_0. \tag{11}$$

It follows that the solution to problem (11) is feasible for problem (9), although it will be suboptimal in general. Our interest in problem (11) stems from the fact that it can be solved in closed form:

Theorem 1. *Let* $\mathbf{\Phi} \in \mathbb{C}^{N_\mathrm{r}\times N_\mathrm{s}}$ *and* $\mathbf{\Gamma} \in \mathbb{C}^{N_\mathrm{t}\times N_\mathrm{s}}$ *respectively comprise the* N_s *left and right singular vectors of the channel matrix* $\boldsymbol{H}$ *corresponding to the* N_s *largest singular values. Then the solution to problem* (11) *is given by*

$$\boldsymbol{F} = \sqrt{p_0}\mathbf{\Gamma}\boldsymbol{Q}, \qquad \boldsymbol{W} = \mathbf{\Phi}\boldsymbol{T}, \tag{12}$$

with $\boldsymbol{Q} \in \mathbb{C}^{N_\mathrm{s}\times N_\mathrm{s}}$ *an arbitrary unitary matrix, and* $\boldsymbol{T} \in \mathbb{C}^{N_\mathrm{s}\times N_\mathrm{s}}$ *an arbitrary invertible matrix.*

The proof is in Appendix B. Note that the optimum precoder for problem (11) is semiunitary with uniform power allocation across the N_s data streams. If one is to take such precoder as an approximate, suboptimal solution to problem (9), then performance can be improved by optimizing such power allocation. Specifically, suppose that, in view of Theorem 1, we take $\boldsymbol{W} = \mathbf{\Phi}$, and $\boldsymbol{F} = \mathbf{\Gamma}\mathbf{\Delta}$ with $\mathbf{\Delta} = \mathrm{diag}\{\,\delta_1 \cdots \delta_{N_\mathrm{s}}\,\}$, and then maximize $\mathcal{R}$ in terms of $\mathbf{\Delta}$ subject to the per-antenna power constraints. Then the problem becomes

$$\begin{aligned}&\max_{\mathbf{\Delta}} \mathcal{R}(\mathbf{\Gamma\Delta}, \mathbf{\Phi}) = \log_2\left|\boldsymbol{I}_{N_\mathrm{s}} + \frac{\rho}{N_\mathrm{s}}\mathbf{\Sigma}^2\mathbf{\Delta}^2\right| \\ &\quad\text{s. to} \qquad \boldsymbol{e}_j^*\mathbf{\Gamma}\mathbf{\Delta}^2\mathbf{\Gamma}^*\boldsymbol{e}_j \le p_j, \quad j = 1,\dots,N_\mathrm{t},\end{aligned} \tag{13}$$

where $\mathbf{\Sigma} = \mathrm{diag}\{\,\sigma_1 \cdots \sigma_{N_\mathrm{s}}\,\}$ comprises the N_s largest singular values of $\boldsymbol{H}$. Letting γ_{jk} denote the (j,k)-th element of $\mathbf{\Gamma}$, (13) can be explicitly written as

$$\begin{aligned}&\max_{\{\delta_k^2\}} \sum_{k=1}^{N_\mathrm{s}} \log_2\left(1 + \frac{\rho\sigma_k^2}{N_\mathrm{s}}\delta_k^2\right) \\ &\quad\text{s. to} \quad \begin{cases} \sum_{k=1}^{N_\mathrm{s}} |\gamma_{jk}|^2\delta_k^2 \le p_j, & j = 1,\dots,N_\mathrm{t}, \\ \delta_k^2 \ge 0, & k = 1,\dots,N_\mathrm{s}.\end{cases}\end{aligned} \tag{14}$$

Since problem (14) is convex, the corresponding power allocation coefficients $\{\delta_k\}$ can be efficiently found. The standard waterfilling problem is obtained if the per-antenna constraints in (14) are replaced by a total power constraint.

V. Hybrid precoder design

The fact that any orthonormal basis of the subspace spanned by the columns of $\mathbf{\Gamma}$ is optimal for problem (11) as per Theorem 1 motivates the following approach to the design of the hybrid precoder $\boldsymbol{F} = \boldsymbol{F}_\mathrm{RF}\boldsymbol{F}_\mathrm{BB}$:

$$\begin{aligned}&\max_{\boldsymbol{F}_\mathrm{BB},\boldsymbol{F}_\mathrm{RF}} \|\mathbf{\Gamma}^*\boldsymbol{F}_\mathrm{RF}\boldsymbol{F}_\mathrm{BB}\|_F^2 \\ &\quad\text{s. to} \quad \begin{cases} \boldsymbol{F}_\mathrm{RF} \in \mathcal{M}^{N_\mathrm{t}\times L_\mathrm{t}}, \\ \boldsymbol{e}_j^*\boldsymbol{F}_\mathrm{RF}\boldsymbol{F}_\mathrm{BB}\boldsymbol{F}_\mathrm{BB}^*\boldsymbol{F}_\mathrm{RF}^*\boldsymbol{e}_j \le p_j, \quad j = 1,\dots,N_\mathrm{t},\end{cases}\end{aligned} \tag{15}$$

which incorporates the hardware-specific as well as the per-antenna power constraints. Note that the objective in (15) does not change if we replace $\mathbf{\Gamma}$ with $\mathbf{\Gamma}\boldsymbol{Q}$, with $\boldsymbol{Q}$ any unitary matrix. In [3], it was shown that, under certain aproximations, maximizing $\|\mathbf{\Gamma}^*\boldsymbol{F}_\mathrm{RF}\boldsymbol{F}_\mathrm{BB}\|_F^2$ was equivalent to maximizing the mutual information. As also mentioned in [3], this term is related to the chordal distance between $\mathbf{\Gamma}$ and $\boldsymbol{F}_\mathrm{RF}\boldsymbol{F}_\mathrm{BB}$ in the Grassmann manifold when $\boldsymbol{F}_\mathrm{RF}\boldsymbol{F}_\mathrm{BB}$ is made semiunitary.

Problem (15) is intractable due to the hardware constraints. To proceed, we obtain first a reasonable approximation for the RF precoder, and then optimize the baseband precoder. As shown in [4], a sensible choice for the RF precoder is the projection of the channel right singular vectors onto $\mathcal{M}^{N_\mathrm{t}\times L_\mathrm{t}}$. Specifically, let $\tilde{\mathbf{\Gamma}} \in \mathbb{C}^{N_\mathrm{t}\times L_\mathrm{t}}$ comprise the L_t right singular vectors of $\boldsymbol{H}$ corresponding to the L_t largest singular values, and let $\tilde{\gamma}_{jk}$ denote the (j,k)-th element of $\tilde{\mathbf{\Gamma}}$. Then we set

$$(\boldsymbol{F}_\mathrm{RF})_{jk} = \frac{\tilde{\gamma}_{jk}}{|\tilde{\gamma}_{jk}|}, \qquad \begin{cases} j = 1,\dots,N_\mathrm{t}, \\ k = 1,\dots,L_\mathrm{t}.\end{cases} \tag{16}$$

With this choice for the RF precoder $\boldsymbol{F}_\mathrm{RF}$, we propose to find $\boldsymbol{F}_\mathrm{BB}$ according to the following design:

$$\begin{aligned}&\max_{\boldsymbol{F}_\mathrm{BB}} \|\mathbf{\Gamma}^*\boldsymbol{F}_\mathrm{RF}\boldsymbol{F}_\mathrm{BB}\|_F^2 \\ &\quad\text{s. to} \qquad \boldsymbol{e}_j^*\boldsymbol{F}_\mathrm{RF}\boldsymbol{F}_\mathrm{BB}\boldsymbol{F}_\mathrm{BB}^*\boldsymbol{F}_\mathrm{RF}^*\boldsymbol{e}_j \le p_j, \quad j = 1,\dots,N_\mathrm{t}.\end{aligned} \tag{17}$$

An approximate solution to (17) can be found as follows. First, consider an SVD $\boldsymbol{F}_\mathrm{BB} = \boldsymbol{U}_F\mathbf{\Sigma}_F\boldsymbol{V}_F^*$, with $\boldsymbol{U}_F \in \mathbb{C}^{L_\mathrm{t}\times N_\mathrm{s}}$ and $\mathbf{\Sigma}_F, \boldsymbol{V}_F \in \mathbb{C}^{N_\mathrm{s}\times N_\mathrm{s}}$, so that $\boldsymbol{F}_\mathrm{BB}\boldsymbol{F}_\mathrm{BB}^* = \boldsymbol{U}_F\mathbf{\Sigma}_F^2\boldsymbol{U}_F^*$. Then let $\boldsymbol{A} = \boldsymbol{F}_\mathrm{RF}^*\mathbf{\Gamma} \in \mathbb{C}^{L_\mathrm{t}\times N_\mathrm{s}}$, so that the objective in (17) becomes $\|\boldsymbol{A}^*\boldsymbol{F}_\mathrm{BB}\|_F^2 = \mathrm{tr}[\boldsymbol{A}^*\boldsymbol{F}_\mathrm{BB}\boldsymbol{F}_\mathrm{BB}^*\boldsymbol{A}]$. Since neither the objective nor the constraints in (17) depend on $\boldsymbol{V}_F$, we can take $\boldsymbol{V}_F = \boldsymbol{I}_{N_\mathrm{s}}$ without loss of optimality.

Now let $\boldsymbol{A} = \boldsymbol{U}_A\mathbf{\Sigma}_A\boldsymbol{V}_A^*$ be an SVD of $\boldsymbol{A}$, with $\boldsymbol{U}_A \in \mathbb{C}^{L_\mathrm{t}\times N_\mathrm{s}}$ and $\mathbf{\Sigma}_A, \boldsymbol{V}_A \in \mathbb{C}^{N_\mathrm{s}\times N_\mathrm{s}}$. Then

$$\|\boldsymbol{A}^*\boldsymbol{F}_\mathrm{BB}\|_F^2 = \mathrm{tr}[\boldsymbol{A}\boldsymbol{A}^*\boldsymbol{F}_\mathrm{BB}\boldsymbol{F}_\mathrm{BB}^*] \le \mathrm{tr}[\mathbf{\Sigma}_A^2\mathbf{\Sigma}_F^2], \tag{18}$$

where the last step in (18) follows from Von Neumann's trace inequality [19] (singular values in $\mathbf{\Sigma}_A$ and $\mathbf{\Sigma}_F$ are assumed sorted in descending order). Equality is achieved in (18) if $\boldsymbol{U}_F = \boldsymbol{U}_A$. Thus, it is reasonable to choose the baseband precoder as $\boldsymbol{F}_\mathrm{BB} = \boldsymbol{U}_A\mathbf{\Sigma}_F$, and then find $\mathbf{\Sigma}_F$ by solving

$$\begin{aligned}&\max_{\mathbf{\Sigma}_F} \mathrm{tr}[\mathbf{\Sigma}_A^2\mathbf{\Sigma}_F^2] \\ &\quad\text{s. to} \qquad \boldsymbol{e}_j^*\boldsymbol{F}_\mathrm{RF}\boldsymbol{U}_A\mathbf{\Sigma}_F^2(\boldsymbol{F}_\mathrm{RF}\boldsymbol{U}_A)^*\boldsymbol{e}_j \le p_j, \quad j = 1,\dots,N_\mathrm{t}.\end{aligned} \tag{19}$$

If we let $\boldsymbol{B} = \boldsymbol{F}_\mathrm{RF}\boldsymbol{U}_A$, with elements b_{jk}, and

$$\mathbf{\Sigma}_A = \mathrm{diag}\{\;\sigma_{A,1}\quad \sigma_{A,2}\quad \cdots\quad \sigma_{A,N_\mathrm{s}}\;\}, \tag{20}$$

$$\mathbf{\Sigma}_F = \mathrm{diag}\{\;\sigma_{F,1}\quad \sigma_{F,2}\quad \cdots\quad \sigma_{F,N_\mathrm{s}}\;\}, \tag{21}$$

then (19) can be explicitly written as

$$\begin{aligned}&\max_{\{\sigma_{F,k}^2\}} \sum_{k=1}^{N_\mathrm{s}} \sigma_{A,k}^2\sigma_{F,k}^2 \\ &\quad\text{s. to} \quad \begin{cases} \sum_{k=1}^{N_\mathrm{s}} |b_{jk}|^2\sigma_{F,k}^2 \le p_j, & j = 1,\dots,N_\mathrm{t}, \\ \sigma_{F,k}^2 \ge 0, & k = 1,\dots,N_\mathrm{s},\end{cases}\end{aligned} \tag{22}$$

which is a linear program in the allocation variables $\sigma_{F,k}^2$.

Note that the proposed design for the baseband precoder $\boldsymbol{F}_\mathrm{BB}$ is not, in general, the exact solution to (17). This is because choosing $\boldsymbol{U}_F = \boldsymbol{U}_A$ is optimal if the per-antenna power constraints are ignored, but it need not be so once they are taken into account.

VI. Hybrid combiner design

To design the combiner $\boldsymbol{W} = \boldsymbol{W}_{\mathrm{RF}}\boldsymbol{W}_{\mathrm{BB}}$, we start from the following two observations. First, in view of Theorem 1, any basis of the N_{s}-dimensional subspace spanned by the columns of $\boldsymbol{\Phi}$ is optimal for problem (11). Second, by choosing the combiner to have orthonormal columns, there is no loss of optimality in terms of spectral efficiency. These suggest the following design for the hybrid combiner:

$$\max_{\boldsymbol{W}_{\mathrm{BB}},\boldsymbol{W}_{\mathrm{RF}}} \|\boldsymbol{\Phi}^*\boldsymbol{W}_{\mathrm{RF}}\boldsymbol{W}_{\mathrm{BB}}\|_F^2 \quad \text{s. to} \quad \begin{cases} \boldsymbol{W}_{\mathrm{RF}} \in \mathcal{M}^{N_{\mathrm{r}}\times L_{\mathrm{r}}}, \\ (\boldsymbol{W}_{\mathrm{RF}}\boldsymbol{W}_{\mathrm{BB}})^*(\boldsymbol{W}_{\mathrm{RF}}\boldsymbol{W}_{\mathrm{BB}}) = \boldsymbol{I}_{N_{\mathrm{s}}}. \end{cases} \tag{23}$$

Using a similar approach to that in Sec. V, we first obtain a reasonable approximation for the RF combiner $\boldsymbol{W}_{\mathrm{RF}}$, and then optimize the baseband combiner $\boldsymbol{W}_{\mathrm{BB}}$. Thus, let $\tilde{\boldsymbol{\Phi}} \in \mathbb{C}^{N_{\mathrm{r}}\times L_{\mathrm{r}}}$ comprise the L_{r} left singular vectors of $\boldsymbol{H}$ corresponding to the L_{r} largest singular values, and let $\tilde{\phi}_{jk}$ be the (j,k)-th element of $\tilde{\boldsymbol{\Phi}}$. Then

$$(\boldsymbol{W}_{\mathrm{RF}})_{jk} = \frac{\tilde{\phi}_{jk}}{|\tilde{\phi}_{jk}|}, \quad \begin{cases} j = 1,\ldots,N_{\mathrm{r}}, \\ k = 1,\ldots,L_{\mathrm{r}}. \end{cases} \tag{24}$$

With this choice for $\boldsymbol{W}_{\mathrm{RF}}$, we find now $\boldsymbol{W}_{\mathrm{BB}}$ by solving

$$\max_{\boldsymbol{W}_{\mathrm{BB}}} \|\boldsymbol{\Phi}^*\boldsymbol{W}_{\mathrm{RF}}\boldsymbol{W}_{\mathrm{BB}}\|_F^2 \quad \text{s. to} \quad (\boldsymbol{W}_{\mathrm{RF}}\boldsymbol{W}_{\mathrm{BB}})^*(\boldsymbol{W}_{\mathrm{RF}}\boldsymbol{W}_{\mathrm{BB}}) = \boldsymbol{I}_{N_{\mathrm{s}}}. \tag{25}$$

The solution to problem (25) is as follows. Consider the SVD $\boldsymbol{W}_{\mathrm{RF}} = \boldsymbol{U}_W\boldsymbol{\Sigma}_W\boldsymbol{V}_W^*$. Then the set of matrices $\boldsymbol{W}_{\mathrm{BB}}$ satisfying the constraint $(\boldsymbol{W}_{\mathrm{RF}}\boldsymbol{W}_{\mathrm{BB}})^*(\boldsymbol{W}_{\mathrm{RF}}\boldsymbol{W}_{\mathrm{BB}}) = \boldsymbol{I}_{N_{\mathrm{s}}}$ is given by $\boldsymbol{W}_{\mathrm{BB}} = \boldsymbol{V}_W\boldsymbol{\Sigma}_W^{-1}\boldsymbol{Z}$, with $\boldsymbol{Z} \in \mathbb{C}^{L_{\mathrm{r}}\times N_{\mathrm{s}}}$ an arbitrary matrix with orthonormal columns. Therefore,

$$\|\boldsymbol{\Phi}^*\boldsymbol{W}_{\mathrm{RF}}\boldsymbol{W}_{\mathrm{BB}}\|_F^2 = \|\boldsymbol{\Phi}^*\boldsymbol{U}_W\boldsymbol{Z}\|_F^2, \tag{26}$$

which is maximized subject to $\boldsymbol{Z}^*\boldsymbol{Z} = \boldsymbol{I}_{N_{\mathrm{s}}}$ when $\boldsymbol{Z}$ spans the same subspace as the N_{s} left singular vectors of $\boldsymbol{U}_W^*\boldsymbol{\Phi}$ corresponding to the N_{s} largest singular values.

The overall proposed design is summarized in Algorithm 1.

Algorithm 1 Hybrid precoder and combiner design with per-antenna power constraints

Precoder:

- Set $\tilde{\boldsymbol{\Gamma}} = (\tilde{\gamma}_{jk}) \leftarrow L_{\mathrm{t}}$ dominant right singular vectors of $\boldsymbol{H}$
- Compute RF precoder $\boldsymbol{F}_{\mathrm{RF}}$ by (16)
- Set $\boldsymbol{\Gamma} \leftarrow N_{\mathrm{s}}$ dominant right singular vectors of $\boldsymbol{H}$
- Set $\boldsymbol{A} = \boldsymbol{F}_{\mathrm{RF}}^*\boldsymbol{\Gamma}$ with SVD $\boldsymbol{A} = \boldsymbol{U}_A\boldsymbol{\Sigma}_A\boldsymbol{V}_A^*$
- Set $\boldsymbol{B} = (b_{jk}) = \boldsymbol{F}_{\mathrm{RF}}\boldsymbol{U}_A$
- Compute $\boldsymbol{\Sigma}_F$ by solving the linear program (22)
- Compute baseband precoder $\boldsymbol{F}_{\mathrm{BB}} = \boldsymbol{U}_A\boldsymbol{\Sigma}_F$

Combiner:

- Set $\tilde{\boldsymbol{\Phi}} = (\tilde{\phi}_{jk}) \leftarrow L_{\mathrm{r}}$ dominant left singular vectors of $\boldsymbol{H}$
- Compute RF combiner $\boldsymbol{W}_{\mathrm{RF}}$ by (24)
- SVD: $\boldsymbol{W}_{\mathrm{RF}} = \boldsymbol{U}_W\boldsymbol{\Sigma}_W\boldsymbol{V}_W^*$
- Set $\boldsymbol{Z} \leftarrow N_{\mathrm{s}}$ dominant left singular vectors of $\boldsymbol{U}_W^*\boldsymbol{\Phi}$
- Compute baseband combiner $\boldsymbol{W}_{\mathrm{BB}} = \boldsymbol{V}_W\boldsymbol{\Sigma}_W^{-1}\boldsymbol{Z}$

VII. Performance Evaluation

In this section we provide simulation based numerical evidence for the performance of the proposed hybrid precoding and combining methods with per-antenna power constraints, highlighting the tradeoff between spectral efficiency and per-antenna power consumption.

We consider the narrowband clustered channel model from [3], with N_{cl} scattering clusters, each of which contributing N_{ray} propagation paths. The channel matrix is then given by

$$\boldsymbol{H} = \sqrt{\frac{N_{\mathrm{t}}N_{\mathrm{r}}}{N_{\mathrm{cl}}N_{\mathrm{ray}}}}\sum_{i=1}^{N_{\mathrm{cl}}}\sum_{\ell=1}^{N_{\mathrm{ray}}}\beta_{i,\ell}\boldsymbol{a}_{\mathrm{r}}(\phi_{i,\ell}^{\mathrm{r}})\boldsymbol{a}_{\mathrm{t}}^*(\phi_{i,\ell}^{\mathrm{t}}), \tag{27}$$

with $\beta_{i,\ell}$ the complex gain of the ℓ^{th} ray in the i^{th} cluster, and $\boldsymbol{a}_{\mathrm{t}}(\phi_{i,\ell}^{\mathrm{t}})$ and $\boldsymbol{a}_{\mathrm{r}}(\phi_{i,\ell}^{\mathrm{r}})$ the antenna array steering and response vectors at the transmitter and receiver, respectively, evaluated at the corresponding azimuth angles of departure or arrival. In the simulations, we take $N_{\mathrm{cl}} = 6$ clusters with equal powers and $N_{\mathrm{ray}} = 8$ paths per cluster. The path gains are independently drawn from a circular complex Gaussian distribution. The angles of departure and arrival are random, with uniformly distributed mean cluster angle and angular spreads of 7.5°. Uniform linear arrays (ULA) are assumed at the transmitter and receiver, with $N_{\mathrm{t}} = 64$ and $N_{\mathrm{r}} = 16$ antennas respectively. The number of RF chains are $L_{\mathrm{t}} = L_{\mathrm{r}} = 4$. Results are averaged over 100 channel realizations.

We compare the proposed hybrid design under per-antenna power constraints (PPC) as given by Algorithm 1 with two all-digital designs. The first one assumes a total power constraint (TPC), the precoder and combiner are taken as the dominant singular vectors of the channel, and power allocation across streams is performed via waterfilling. In the second design we use Pi's algorithm from [13] to design the precoder under per-antenna constraints, and then take the combiner from the channel's dominant left singular vectors. For the PPC designs, a uniform power constraint $p_j = P_a \; \forall j$ is placed at all antennas, whereas for the TPC design the total available power is $N_{\mathrm{t}}P_a$.

Fig. 2 shows the performance of the three designs in terms of spectral efficiency vs. the SNR ρ, for different number of data streams N_{s}. As observed in [13], the all-digital solution obtained by Pi's PPC algorithm performs very close to the TPC waterfilling solution. The proposed PPC hybrid design achieves spectral efficiencies close to those of Pi's method, with a small performance loss which increases with the number of data streams.

Fig. 3 shows the complementary cumulative distribution of the power consumed by a given antenna, for both the TPC waterfilling design and the proposed PPC hybrid approach (for Pi's method, the power at each antenna is exactly P_a, as shown in [13, Th. 1]). It is seen that the proposed hybrid design always meets the per-antenna constraints but not necessarily with equality, i.e., there can be antennas whose amplifiers do not deliver their maximum available power, especially for low values of N_{s}; when number of data streams is the same as the number of RF chains (4 in this example), all antennas are seen

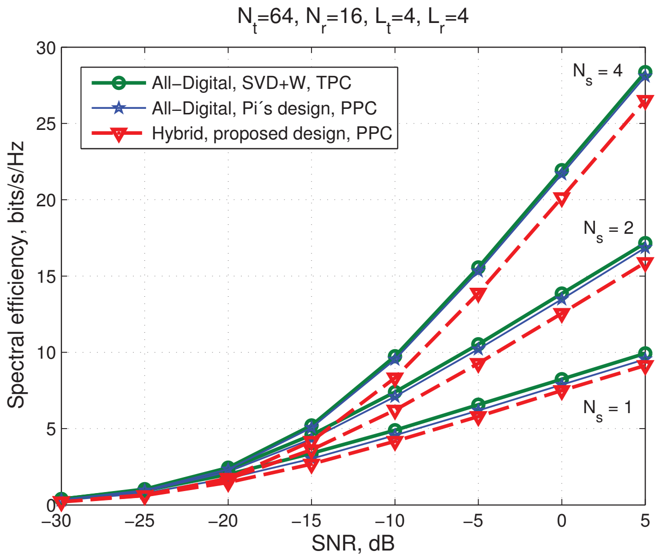

Fig. 2. Spectral efficiency for the different designs.

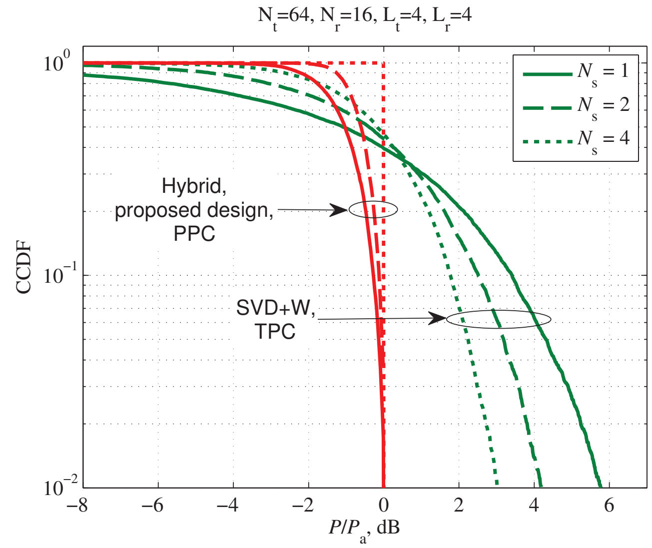

Fig. 3. Complementary cumulative distribution of the power at any given antenna. The SNR is 0 dB.

to transmit at maximum power. The TPC waterfilling design yields a power distribution with larger spread across antennas, with peak value decreasing as N_{s} increases. For example, the probability of a given antenna transmitting 3 dB above P_a is 0.13, 0.06, and 0.01 for $N_{\mathrm{s}} = 1$, 2, and 4 respectively. From Fig. 3, one can estimate the performance loss incurred if the TPC waterfilling design was to be directly scaled down in order to meet the per-antenna power constraints; for instance, if a probability of 0.01 for a given antenna not fulfilling the constraint is desired, the transmit power would have to be backed off by approximately 6, 4, and 3 dB respectively for $N_{\mathrm{s}} = 1$, 2, and 4, meaning that the corresponding "SVD+W" curves in Fig. 2 would shift to the right by the same amounts. This shows the benefits of taking individual per-antenna constraints into account at the design stage.

VIII. Conclusion

We have developed a closed-form approximation for the digital precoder and combiner maximizing spectral efficiency in a MIMO system with per-antenna power constraints. Then we considered a mmWave MIMO system implemented with a hybrid architecture and developed a heuristic algorithm for the design of the hybrid precoder and combiner approximating the all-digital solution. Simulations show that hybrid designs with per-antenna power constraints achieve spectral efficiencies close to that of the all-digital solution. We also studied the power distribution over the antennas resulting from the hybrid design, finding that the per-antenna constraints are always met, but not necessarily with equality. The importance of considering per-antenna power constraints at the design stage has been shown.

Appendix A: Proof of Lemma 1

Let $(\boldsymbol{F}_0, \boldsymbol{W}_0)$ maximize $\mathcal{R}(\boldsymbol{F}, \boldsymbol{W})$ in (5) subject to the per-antenna power constraints (6), and consider the SVD $\boldsymbol{W}_0 = \boldsymbol{U}_0\boldsymbol{\Sigma}_0\boldsymbol{V}_0^*$. Now fix in (5) the combiner to $\boldsymbol{W}_0$ and consider the resulting function of $\boldsymbol{F}$:

$$\mathcal{R}(\boldsymbol{F}, \boldsymbol{W}_0) = \log_2 \left| \boldsymbol{I}_{N_{\mathrm{s}}} + \frac{\rho}{N_{\mathrm{s}}} \boldsymbol{F}^*\boldsymbol{H}^*\boldsymbol{U}_0\boldsymbol{U}_0^*\boldsymbol{H}\boldsymbol{F} \right|, \tag{28}$$

which is just the mutual information for a channel with matrix $\boldsymbol{U}_0^*\boldsymbol{H}$. By the same argument as that in [13, Th. 1], the optimum precoder $\boldsymbol{F}_0$, which maximizes (28) under (6), must satisfy such constraints with equality. $\square$

Appendix B: Proof of Theorem 1

Considering the SVDs of the precoder and combiner,

$$\boldsymbol{F} = \boldsymbol{U}_F\boldsymbol{\Sigma}_F\boldsymbol{V}_F^*, \quad \boldsymbol{W} = \boldsymbol{U}_W\boldsymbol{\Sigma}_W\boldsymbol{V}_W^*, \tag{29}$$

then it is found that the spectral efficiency $\mathcal{R}(\boldsymbol{F}, \boldsymbol{W})$ in (5) is a function of $\boldsymbol{U}_F$, $\boldsymbol{\Sigma}_F$ and $\boldsymbol{U}_W$ alone:

$$\mathcal{R}(\boldsymbol{F}, \boldsymbol{W}) = \log_2 \left| \boldsymbol{I}_{N_{\mathrm{s}}} + \frac{\rho}{N_{\mathrm{s}}} \boldsymbol{U}_W^*\boldsymbol{H}\boldsymbol{U}_F\boldsymbol{\Sigma}_F^2\boldsymbol{U}_F^*\boldsymbol{H}^*\boldsymbol{U}_W \right|, \tag{30}$$

where the cyclic property of the determinant $|\boldsymbol{I} + \boldsymbol{A}\boldsymbol{B}| = |\boldsymbol{I} + \boldsymbol{B}\boldsymbol{A}|$ has been used. Thus, we must maximize (30) subject to

$$\boldsymbol{U}_W^*\boldsymbol{U}_W = \boldsymbol{I}_{N_{\mathrm{s}}}, \quad \boldsymbol{U}_F^*\boldsymbol{U}_F = \boldsymbol{I}_{N_{\mathrm{s}}}, \quad p_0\boldsymbol{I}_{N_{\mathrm{s}}} - \boldsymbol{\Sigma}_F^2 \geq \boldsymbol{0}. \tag{31}$$

Let now

$$\boldsymbol{\Sigma}_F = \mathrm{diag}\{ \rho_1 \quad \rho_2 \quad \cdots \quad \rho_{N_{\mathrm{s}}} \}, \tag{32}$$

$$\boldsymbol{X} = \left(\frac{\rho}{N_{\mathrm{s}}} \boldsymbol{U}_F^*\boldsymbol{H}^*\boldsymbol{U}_W\boldsymbol{U}_W^*\boldsymbol{H}\boldsymbol{U}_F \right)^{-1}, \tag{33}$$

so that (30) can be rewritten as

$$\mathcal{R}(\boldsymbol{F}, \boldsymbol{W}) = \log_2 \left| \boldsymbol{I}_{N_{\mathrm{s}}} + \boldsymbol{X}^{-1}\boldsymbol{\Sigma}_F^2 \right| \tag{34}$$

$$= \log_2 \left| \boldsymbol{X}^{-1} \right| + \log_2 \left| \boldsymbol{X} + \boldsymbol{\Sigma}_F^2 \right|. \tag{35}$$

Denoting $\boldsymbol{X}_k = \boldsymbol{X} + \sum_{i \neq k} \rho_i \boldsymbol{e}_i \boldsymbol{e}_i^*$, one has

$$\begin{aligned} \left|\boldsymbol{X} + \boldsymbol{\Sigma}_F^2\right| &= \left|\boldsymbol{X} + \sum_{i=1}^{N_\mathrm{s}} \rho_i^2 \boldsymbol{e}_i \boldsymbol{e}_i^*\right| \qquad (36) \\ &= \left(1 + \rho_k^2 \boldsymbol{e}_k^* \boldsymbol{X}_k^{-1} \boldsymbol{e}_k\right) |\boldsymbol{X}_k|. \qquad (37) \end{aligned}$$

Since $\boldsymbol{X}_k$ does not depend on ρ_k, the value of $\rho_k^2 \in [0, p_0]$ maximizing $\left|\boldsymbol{X} + \boldsymbol{\Sigma}_F^2\right|$ is $\rho_k^2 = p_0$. This is true for every $k = 1, \ldots, N_\mathrm{s}$, hence $\boldsymbol{\Sigma}_F^2 = p_0 \boldsymbol{I}_{N_\mathrm{s}}$ is optimal, yielding

$$\mathcal{R}(\boldsymbol{F}, \boldsymbol{W}) = \log_2 \left|\boldsymbol{I}_{N_\mathrm{s}} + \frac{\rho p_0}{N_\mathrm{s}} \boldsymbol{U}_W^* \boldsymbol{H} \boldsymbol{U}_F \boldsymbol{U}_F^* \boldsymbol{H}^* \boldsymbol{U}_W\right|. \qquad (38)$$

Let $\boldsymbol{C} = \frac{\rho p_0}{N_\mathrm{s}} \boldsymbol{H} \boldsymbol{U}_F \boldsymbol{U}_F^* \boldsymbol{H}^*$, and consider the maximization of (38) with respect to $\boldsymbol{U}_W$:

$$\begin{aligned} \mathcal{R}(\boldsymbol{F}, \boldsymbol{W}) &= \log_2 \left|\boldsymbol{I}_{N_\mathrm{s}} + \boldsymbol{U}_W^* \boldsymbol{C} \boldsymbol{U}_W\right| \qquad (39) \\ &= \log_2 \left|\boldsymbol{I}_{N_\mathrm{r}} + \boldsymbol{U}_W \boldsymbol{U}_W^* \boldsymbol{C}\right|. \qquad (40) \end{aligned}$$

For $\boldsymbol{A} \in \mathbb{C}^{n \times n}$ Hermitian, let $\lambda_1(\boldsymbol{A}) \geq \lambda_2(\boldsymbol{A}) \geq \cdots \geq \lambda_n(\boldsymbol{A})$ be its ordered eigenvalues. Using Lemma 3 from [20],

$$\begin{aligned} \left|\boldsymbol{I}_{N_\mathrm{r}} + \boldsymbol{U}_W \boldsymbol{U}_W^* \boldsymbol{C}\right| &\leq \prod_{i=1}^{N_\mathrm{r}} \left(1 + \lambda_i(\boldsymbol{U}_W \boldsymbol{U}_W^*) \lambda_i(\boldsymbol{C})\right) \qquad (41) \\ &= \prod_{i=1}^{N_\mathrm{s}} \left(1 + \lambda_i(\boldsymbol{C})\right), \qquad (42) \end{aligned}$$

where the second step follows from the fact that $\lambda_i(\boldsymbol{U}_W \boldsymbol{U}_W^*) = 1$ for $1 \leq i \leq N_\mathrm{s}$ and zero otherwise. The upper bound is achieved if the columns of $\boldsymbol{U}_W$ constitute an orthonormal basis for the subspace spanned by the N_s dominant eigenvectors of $\boldsymbol{C}$.

It remains to maximize (42) with respect to $\boldsymbol{U}_F$. Note that

$$\begin{aligned} \prod_{i=1}^{N_\mathrm{s}} \left(1 + \lambda_i(\boldsymbol{C})\right) &\leq \prod_{i=1}^{N_\mathrm{r}} \left(1 + \lambda_i(\boldsymbol{C})\right) \\ &= \left|\boldsymbol{I}_{N_\mathrm{r}} + \boldsymbol{C}\right| \\ &= \left|\boldsymbol{I}_{N_\mathrm{r}} + \frac{\rho p_0}{N_\mathrm{s}} \boldsymbol{H} \boldsymbol{U}_F \boldsymbol{U}_F^* \boldsymbol{H}^*\right| \\ &= \left|\boldsymbol{I}_{N_\mathrm{t}} + \frac{\rho p_0}{N_\mathrm{s}} \boldsymbol{U}_F \boldsymbol{U}_F^* \boldsymbol{H}^* \boldsymbol{H}\right| \\ &\leq \prod_{i=1}^{N_\mathrm{t}} \left(1 + \frac{\rho p_0}{N_\mathrm{s}} \lambda_i(\boldsymbol{U}_F \boldsymbol{U}_F^*) \lambda_i(\boldsymbol{H}^* \boldsymbol{H})\right) \\ &= \prod_{i=1}^{N_\mathrm{s}} \left(1 + \frac{\rho p_0}{N_\mathrm{s}} \lambda_i(\boldsymbol{H}^* \boldsymbol{H})\right), \qquad (43) \end{aligned}$$

where we have applied again [20, Lemma 3] and the fact that the only nonzero eigenvalue of $\boldsymbol{U}_F \boldsymbol{U}_F^*$ is 1, with multiplicity N_s. The upper bound in (43) is achieved if the columns of $\boldsymbol{U}_F$ span the subspace of the N_s dominant right singular vectors of $\boldsymbol{H}$, i.e., $\boldsymbol{U}_F = \boldsymbol{\Gamma} \boldsymbol{Q}$ for any unitary $\boldsymbol{Q} \in \mathbb{C}^{N_\mathrm{s} \times N_\mathrm{s}}$. This yields $\boldsymbol{H} \boldsymbol{U}_F \boldsymbol{U}_F^* \boldsymbol{H}^* = \boldsymbol{\Phi} \boldsymbol{\Sigma}^2 \boldsymbol{\Phi}^*$, where $\boldsymbol{\Phi} \in \mathbb{C}^{N_\mathrm{r} \times N_\mathrm{s}}$ comprises the N_s dominant left singular vectors of $\boldsymbol{H}$, and $\boldsymbol{\Sigma} \in \mathbb{C}^{N_\mathrm{s} \times N_\mathrm{s}}$ is diagonal with the corresponding N_s largest singular values. Hence, the optimum $\boldsymbol{U}_W$ is of the form $\boldsymbol{U}_W = \boldsymbol{\Phi} \boldsymbol{R}$ for any $\boldsymbol{R} \in \mathbb{C}^{N_\mathrm{s} \times N_\mathrm{s}}$ unitary. The maximum value of $\mathcal{R}$ is given by

$$\mathcal{R}_\star = \left|\boldsymbol{I}_{N_\mathrm{s}} + \frac{\rho p_0}{N_\mathrm{s}} \boldsymbol{\Sigma}^2\right|. \qquad (44)$$

This concludes the proof. $\square$

References

[1] A. Alkhateeb, J. Mo, N. González-Prelcic, and R. W. Heath Jr., "MIMO precoding and combining solutions for millimeter wave systems," *IEEE Commun. Mag.,* vol. 52, no. 12, pp. 122–131, 2014.

[2] R. W. Heath Jr., N. González-Prelcic, S. Rangan, W. Roh, and A. Sayeed, "An overview of signal processing techniques for millimeter wave MIMO systems," *IEEE J. Special Topics Signal Process.,* Apr. 2016.

[3] O. El Ayach, S. Rajagopal, S. Abu-Surra, Z. Pi, R. W. Heath, Jr., "Spatially sparse precoding in mmWave MIMO systems," *IEEE Trans. Wireless Commun.,* vol. 13, no. 3, pp. 1499–1513, Mar. 2014.

[4] R. Méndez-Rial, C. Rusu, N. González-Prelcic, R. W. Heath, Jr., "Dictionary-free hybrid precoders and combiners for mmWave MIMO systems," *IEEE Workshop Signal Process. Adv. Wireless Commun.,* pp. 151–155, 2015.

[5] C. Rusu, R. Méndez-Rial, N. González-Prelcic, and R. W. Heath Jr., "Low complexity hybrid sparse precoding and combining in millimeter wave MIMO systems," *Proc. IEEE Int. Conf. Commun.,* June 2015.

[6] M. Kim and Y. H. Lee, "MSE-based hybrid RF/baseband processing for millimeter-wave communication systems in MIMO interference channels," *IEEE Trans. Veh. Technol.,* vol. 64, no. 6, pp. 2714–2720, June 2015.

[7] J. Singh and S. Ramakrishna, "On the feasibility of codebook-based beamforming in millimeter wave systems with multiple antenna arrays," *IEEE Trans. Wireless Commun.,* vol. 14, no. 5, pp. 2670–2683, May 2015.

[8] E. Zhang and C. Huang, "On achieving optimal rate of digital precoder by RF-baseband codesign for MIMO systems", *IEEE Veh. Technol. Conf. (VTC-Fall),* pp. 1–5, 2014.

[9] F. Sohrabi and W. Yu, "Hybrid digital and analog beamforming design for large-scale MIMO systems," *IEEE Int. Conf. on Acoust., Speech, Signal Process.,* pp. 2929–2933, 2015.

[10] C.-E. Chen, "An iterative hybrid transceiver design algorithm for millimeter wave MIMO systems," *IEEE Wireless Commun. Lett.,* vol. 4, no. 3, pp. 2162–2337, June 2015.

[11] E. Telatar, "Capacity of Multi-antenna Gaussian Channels," *European Trans.Telecommun.,* vol. 10, no. 6, pp. 585–595, Nov.-Dec. 1999.

[12] M. Vu, "MIMO capacity with per-antenna power constraint," *IEEE Global Commun. Conf.,* 2011.

[13] Z. Pi, "Optimal MIMO transmisssion with per-antenna power constraints," *IEEE Global Commun. Conf.,* pp. 2493–2498, 2012.

[14] D. P. Palomar, J. M. Cioffi and M. A. Lagunas, "Joint Tx-Rx beamforming design for multicarrier MIMO channels: A unified framework for convex optimization," *IEEE Trans. Signal Process.,* vol. 51, no. 9, pp. 2381–2401, Sep. 2003.

[15] X. Zheng, Y. Xie, J. Li and P. Stoica, "MIMO Transmit Beamforming Under Uniform Elemental Power Constraint," *IEEE Trans. Signal Process.,* vol. 55, no. 11, pp. 5395–5406, Nov. 2007.

[16] C. C. Weng and P. P. Vaidyanathan, "MIMO transceiver optimization with linear constraints on transmitted signal covariance components," *IEEE Trans. Signal Process.,* vol. 58, no. 1, pp. 458–462, Jan. 2010.

[17] T. Liu, S. Lu and M. Zheng, "Beamforming for per-antenna power constrained downlink SINR optimization," *IEEE Veh. Technol. Conf. (VTC-Spring)*, 2010.

[18] W. Yu and T. Lan, "Downlink beamforming with per-antenna power constraints," *IEEE Workshop Signal Process. Adv. Wireless Commun.,* pp. 1058-1062, 2005.

[19] J. von Neumann, "Some matrix inequalities and metrization of matrix-space," *Tomsk Univ. Rev.,* vol. 1, pp. 286–300 (1937). Reprinted in Collected Works (Pergamon Press, 1962), iv, 205–219.

[20] H. S. Witsenhausen, "A determinant maximization problem occurring in the theory of data communication," *SIAM J. Appl. Math.,* vol. 29, no. 3, pp.515–522, Nov. 1975.